Sensitivity of the Asian summer monsoon to the horizontal resolution: differences between AMIP-type and coupled model experiments

Annalisa Cherchi · Antonio Navarra

Abstract A set of experiments forced with observed SST has been performed with the Echam4 atmospheric GCM at three different horizontal resolutions (T30, T42 and T106). These experiments have been used to study the sensitivity of the simulated Asian summer monsoon (ASM) to the horizontal resolution. The ASM is reasonably well simulated by the Echam4 model at all resolutions. In particular, the low-level westerly flow, that is the dominant manifestation of the Asian summer monsoon, is well captured by the model, and the precipitation is reasonably simulated in intensity and space appearance. The main improvements due to an higher resolution model are associated to regional aspects of the precipitation, for example the Western Ghats precipitation is better reproduced. The interannual variability of precipitation and wind fields in the Asian monsoon region appears to be less affected by an increase in the horizontal resolution than the mean climatology is. A possible reason is that the former is mainly SST-forced. Besides, the availability of experiments at different horizontal resolution realized with the Echam4 model coupled to a global oceanic model allows the possibility to compare these simulations with the experiments previously described. This analysis showed that the coupled model is able to reproduce a realistic monsoon, as the basic dynamics of the phenomenon is captured. The increase of the horizontal resolution of the atmospheric component influences the simulated monsoon with the same characteristics of the forced experiments. Some basic
features of the Asian summer monsoon, as the interannual variability and the connection with ENSO, are further investigated.

1 Introduction

Observational studies (e.g., Shukla 1987; Webster et al. 1998; Annamalai et al. 1999) and numerical model analysis (e.g., Fennessy et al. 1994; Ju and Slingo 1995; Soman and Slingo 1997) have been used in the last decades to study the Asian monsoon and its main features. The monsoon is a complex phenomenon and despite all the studies focused on it, it is still not completely understood. A very important step in the analysis of the Asian monsoon and its characteristics has been the atmospheric model intercomparison project (AMIP; Gates 1992) where a set of experiments forced with observed SST from 1979 to 1994 has been built with different AGCMs. Sperber and Palmer (1996) analyzed all these experiments and among their main results they argued that the simulation of the basic aspects of the monsoon needs further improvements, besides only few models captured the fluctuations between good and poor monsoon seasons in a realistic way.

The Echam4 atmospheric general circulation model is used here to create experiments forced with observed SST from 1956 to 1999 (AMIP-type experiments) interpolated from the HadISST dataset (Rayner et al. 2000). The length of integration allows an accurate study of the climatology and of the interannual variability of the monsoon. Besides, the availability of three different horizontal resolutions (T30,

A. Cherchi (✉) · A. Navarra
Istituto Nazionale di Geofisica e Vulcanologia,
Via Creti 12, Bologna 40128, Italy
e-mail: cherchi@bo.ingv.it

T42 and T106) permits to analyze the sensitivity of the model simulations to the horizontal resolution.

Many studies have focused on the impact of the horizontal resolution on the simulation of the Asian monsoon and its features. Sperber et al. (1994) implemented and analyzed experiments with climatological SST, and they found that higher horizontal resolution is beneficial for the high frequency variability. Other studies have found out a better simulation of the tropical easterly jet over South Asia, Indian Ocean and Africa at higher horizontal resolution (Dümenil and Bauer 1998); while others found a better simulation of precipitation around the Western Ghats and of the strength of the low-level winds over the Bay of Bengal with an higher resolution model (Stendel and Roeckner 1998). A recent study by Kobayashi and Sugi (2004) highlighted that the horizontal resolution alone is not enough to resolve the model biases. For example, they found that the double ITCZ is still present at high resolutions and seems to depend on the convective scheme used.

All those studies never compared the effect of the resolution on the coupled system atmosphere–ocean. Recently, May (2003) focused on the atmospheric model with boundary forcings computed from a coupled atmosphere–ocean system showing that the warm bias on the surface temperature of the coupled model help to better represent the precipitation over India and the position of the ITCZ over the Indian Ocean, but it represents a worse East Asian monsoon.

The Asian monsoon has strong feedbacks with SST and land surface conditions. Coupled atmosphere–ocean models are then supposed to be a very important and useful tool to study the complex behavior of the monsoon. They are able to generate and maintain counterbalanced surface fluxes in time and space depending on the specific characteristics of the model components, this produces internally self-consistent coupled climate simulations compared to atmospheric models integrated with observed SSTs (Meehl 1989). Shukla and Fennessy (1994) performed experiments with a GCM in which the solar forcing of the land and the ocean were incorporated separately in order to investigate the role of the annual march of the SST in the establishment of the monsoon circulation and rainfall. They argued that if a coupled ocean–atmosphere model is not able to simulate the observed annual cycle of the SSTs, the simulated monsoon circulation could be highly deficient.

The simulation and the variability of the Asian summer monsoon (ASM) and its components have been studied with coupled GCMs (e.g., Meehl and Arblaster 1998; Kitoh et al. 1999; Terray et al. 2005).

The mains results are that the coupled models examined tend to reproduce too much precipitation over the Indian Ocean and less over the Indian continent in summer. In particular, Terray et al. (2005) analyzed the Indian summer monsoon (ISM) climatology and interannual variability with the SINTEX coupled model at low resolution (T30) (Gualdi et al. 2003; Guilyardi et al. 2003). They found out that the SINTEX model is able to simulate reasonably well the ISM, in particular the annual cycle of the precipitation over India is realistic, even if the intensity of the precipitation is lower than observed for all the summer season. Furthermore, the cross-Equatorial flow at lower level is in agreement with the reanalysis, even if the Somali jet is not strictly confined near the African coasts, and in the Arabian sea the monsoon is too zonal. From an observational study, Hastenrath (2000) has shown that the upper-level Equatorial easterlies observed during the ISM are more closely associated with the upper branch of the local Hadley circulation than with a thermal circulation driven by the SST gradient along the Equator. Terray et al. (2005) argued that the weakening of the local Hadley cell in the model experiment may play a crucial role in the biases of the precipitation over India in summer.

Among the SINTEX EU project, the SINTEX CGCM has been integrated with the atmosphere at three different horizontal resolutions (T30, T42 and T106). Gualdi et al. (2003) used those experiments to study the impact of the horizontal resolution on the tropical climate variability. In this work we have analyzed them to study the differences on the Asian monsoon simulation imposed by an interactive ocean. Furthermore, to investigate with more details which is the influence of the interaction between atmosphere and ocean we have performed a set of experiments with Echam4 forced by SST obtained as a result of the coupled model simulation. This technique has been used many times in literature (e.g., Latif and Barnett 1994; Kitoh and Arakawa 1999; May 2003; Inatsu and Kimoto 2005) to compare and discuss the differences between AGCM and CGCM simulations.

The amount of precipitation as well as the intensity of the winds are subject to variations among years. The total amount of precipitation in summer (June–September mean) normalized with respect to its standard deviation was defined by Parthasarathy et al. (1992) as all-Indian rainfall (AIR) index. Observations from 1870 to 2000 show that the strength of the ISM in term of precipitation has been highly variable: years with quite intense precipitation are easily followed by drought years. Precipitation data is inhomogeneous and is subject to local effects, so Webster and Yang

(1992) used a dynamic criterion to differentiate between strong and weak monsoons, they defined a dynamical monsoon index (DMI) as the mean JJA shear of the zonal wind ($u_{850} - u_{200}$) averaged over 40°–110°E, Equator – 20°N. That index is a measure of the large-scale monsoon circulation and does not necessarily correspond to the regional rainfall variations represented by AIR (Ju and Slingo 1995). Other monsoon indices have been defined in recent years with the aim to study also the regional aspects of the Asian monsoon, either in terms of the precipitation and of mean winds. The interannual variation of the Indian monsoon is characterized by fluctuations of a regional Hadley circulation, which changes sign from strong to weak monsoon years (Goswami et al. 1999). In that view they have introduced a meridional index MHI, defined as $v_{850} - v_{200}$ averaged in the region 70–110°E 10–30°N in summer.

The interannual variability of the monsoon is modulated, among others boundary forcings, by ENSO (Webster et al. 1998; Sperber et al. 2000). Several studies (e.g., Rasmusson and Carpenter 1983; Zhang et al. 1996; Lau and Nath 2000; Kinter et al. 2002) focused on the relationship between ENSO and the Asian monsoon. In all these studies warm ENSO events were generally related to dry monsoon seasons, with cold ENSO events associated with wet monsoon seasons. The warm episodes of ENSO are associated with a shift in the climatological Walker circulation to the Eastern Pacific. This shift results in enhanced low-level convergence over the Equatorial Indian Ocean and in driving an anomalous Hadley circulation with descent over the Indian continent and decreased monsoon rainfall (Goswami 1998). It has been shown that the ENSO–monsoon interaction has intraseasonal frequency influenced by the MJO (Madden–Julian Oscillation), the monsoon onset, active/break phases of the monsoon itself and westerly wind bursts in the Western Pacific (Webster et al. 1998). An important issue in the connection of monsoon and ENSO is the changes found after 1976 (climate shift), in particular an observational study made by Kinter et al. (2002) evidenced that the relationship between monsoon and ENSO has weakened after 1976. In this study a similar analysis has been made with the results from the AMIP-type experiments.

This study is organized as follow: Sect. 2 describes the model used and the experiments performed. Section 3 includes the analysis of the mean climatology simulated by the models used, as well as a detailed analysis of the main differences associated to the different horizontal resolutions considered. Section 4 is dedicated to the analysis of the new set of experiments

performed forcing the atmospheric model with SST from the coupled model outputs to assess the impact of an interactive ocean. Section 5 describes the interannual variability of the ASM using dynamical index to represent the evolution between strong and weak monsoon years. Section 6 contains the analysis of the connection between monsoon and ENSO. Finally, Sect. 7 is a summary of the main conclusions obtained.

2 Model and observations

2.1 Description of the models and setup of the experiments

The atmospheric general circulation model used, EC-HAM4, represents the 4th generation of the ECHAM (ECmwf HAMburg) atmospheric model developed at the Max Planck Institute für Meteorology in Hamburg (Roeckner et al. 1996). It is a spectral model and the prognostic variables include vorticity, divergence, temperature, surface pressure, water vapour and cloud water. The equations of the model are solved on 19 vertical levels, with the top at 10 hPa. The non-linear terms and the physical processes are computed on a Gaussian grid, with three different horizontal resolutions, T30 (3.75°), T42 (2.128°) and T106 (1.125°). The Echam4 model at different horizontal resolutions has been used to build a set of AMIP-type experiments with prescribed SSTs interannually varying from 1956 to 1999. The SSTs used have been interpolated from the HadISST dataset (Rayner et al. 2000).

Among the SINTEX EU project, the Echam4 GCM has been coupled to OPA8.1 (Madec et al. 1998) by means of Oasis2.4 (Valcke et al. 2000). The coupled system obtained, SINTEX (Gualdi et al. 2003; Guilyardi et al. 2003), is available at three different horizontal resolutions of the atmospheric component.

Ocèan PArallelisée (OPA) is the global ocean circulation model developed at LODYC in Paris (Madec et al. 1998). It is a primitive equation model. The prognostic variables are the three dimensional velocity field and the thermohaline variables. The spatial resolution is about 2° × 1.5°, with a meridional resolution of 0.5° at the Equator. The version of the coupled model used is implemented without flux adjustment.

2.2 Description of the datasets used for comparison

The results of the model experiments have been compared with reanalysis and observations. The CPC merged analysis of precipitation (CMAP) dataset contains global monthly precipitation obtained by

merging gauge data and five kind of satellite estimates with values distributed on global regular gridded fields (grid point 2.5° × 2.5°, Xie and Arkin 1997). The ERA data assimilation system is a special version of the ECMWF system, it contains surface and upper air fields from 1958 to 2002 (for more details see the web site http://www.ecmwf.int). The outgoing longwave radiation (OLR) dataset is that from the National Oceanic and Atmospheric Administration (NOAA) series of satellites (for details Trenberth et al. 2002). The AMIP-type experiments have been forced with interannually varying SST from 1956 to 1999. These fields have been built interpolating the SST from the Hadley centre sea-ice and sea Surface Temperature (HadISST1.1), which consists of monthly SST and sea–ice concentration on a regular grid of 1° × 1° (full details are provided by Rayner et al. 2000).

3 Sensitivity to the horizontal resolution: mean climatology

The monsoon and its main features are generally studied through the analysis of precipitation and wind fields. In Fig. 1 the mean JJA wind at 850 mb is superimposed to the mean JJA OLR. As evidenced in the bottom panel of the figure, one of the most dramatic elements of the ASM is the development of the lower tropospheric Somali Jet in response to the land–sea gradient of large-scale heating (Sperber et al. 2000). The seasonal reverse in direction and the intensification of the low-level wind are well captured by the atmospheric model at all resolutions (Fig. 1a–c). In general even the low-resolution Echam4 GCM has a good representation of the ASM mainly for circulation features (Cherchi and Navarra 2003). The wind at lower levels reverses in direction from easterly to westerly after the Asian monsoon starts. One of the main biases of the atmosphere-only model is the simulation of the south-westerly flow while crossing the Equator. In particular, in the AMIP-type experiments at all resolutions (Fig. 1a–c), the meridional component of the flow is too strong at the Equator. In the coupled model experiments (Fig. 1d–f) this bias is less evident, mainly at higher resolution. In the western tropical Indian Ocean warmer SST, by about 1–1.5°C, with respect to the observations maintains weaker gradient and following Lindzen and Nigam (1987) theory the winds that may be induced are weaker. The feedback between winds and SST prevents a decrease of temperature and an increase of wind intensity.

Figure 2 shows the summer mean meridional wind averaged around the Equator (between – 2.5° and 2.5°

latitude). In some regions, the simulated wind is stronger than observed (i.e. between 20°–40°E, between 60°–80°E and off 140°E). The coupled model winds (dashed lines) are somehow weaker with respect to the AMIP-type experiments results. Along 40°E the main peak is well captured by the AMIP model at high resolution, while along the western coasts of India the simulated wind is much stronger than observed. Comparing the solid and the dashed lines of Fig. 2 it is evident that the main deficiencies in the simulation of the lower tropospheric meridional wind are common to both the models used, but it is noteworthy that the coupled model experiments catch the different peaks of the meridional wind along the Equator in a more realistic way.

After the monsoon onset the low level westerly flow expands from the Indian subcontinent toward China reaching the western Pacific Ocean, as a manifestation of the Western North Pacific High (Wang et al. 2001). This behavior is quite well simulated by the Echam4 model even if the intensity of the winds is larger than in the observations (Fig. 1a–c). The East Asian summer monsoon (EASM) region is characterized by lower level easterly winds from the Pacific Ocean and westerly from the Maritime Continents region, while in the model the main flow comes from the Pacific Ocean producing a somewhat poor simulation of this component of the Asian–Pacific monsoon. In the coupled model experiments (Fig. 1d–f), along South East Asia the wind direction is well simulated, while its intensity is underestimated. In the Western North Pacific region the mean behaviour of lower tropospheric winds is better simulated by the T42 horizontal resolution experiment.

Outgoing longwave radiation pattern is a first guess for convection (Fig. 1, shaded patterns). The areas with OLR < 200 W/m^2 (blue-shaded in the figure) are identified as heating sources and are indicative of convection centres. As OLR minima are indices of persistent deep convection and latent and radiative heat sinks within the troposphere, regions of maxima OLR (values greater than 290 W/m^2 are red-shaded in the figure) indicate radiative loss to space. From the observations (Fig. 1g) two main convection centres may be identified: one is located in the Bay of Bengal and the other in the vicinity of Philippines. At low resolution (Fig. 1a, d), the low values of OLR are located too much south with respect to the observations, with the minima located around 100°E. At T106 resolution the areas with OLR lower than 220 W/m^2 are shifted slightly eastward and southward, assuming a pattern more similar to satellite data (Fig. 1c, f). In all the experiments, the OLR over Indonesia is lower than

OLR (W/m**2) & 850 mb WIND (m/sec)
(Models & observations)
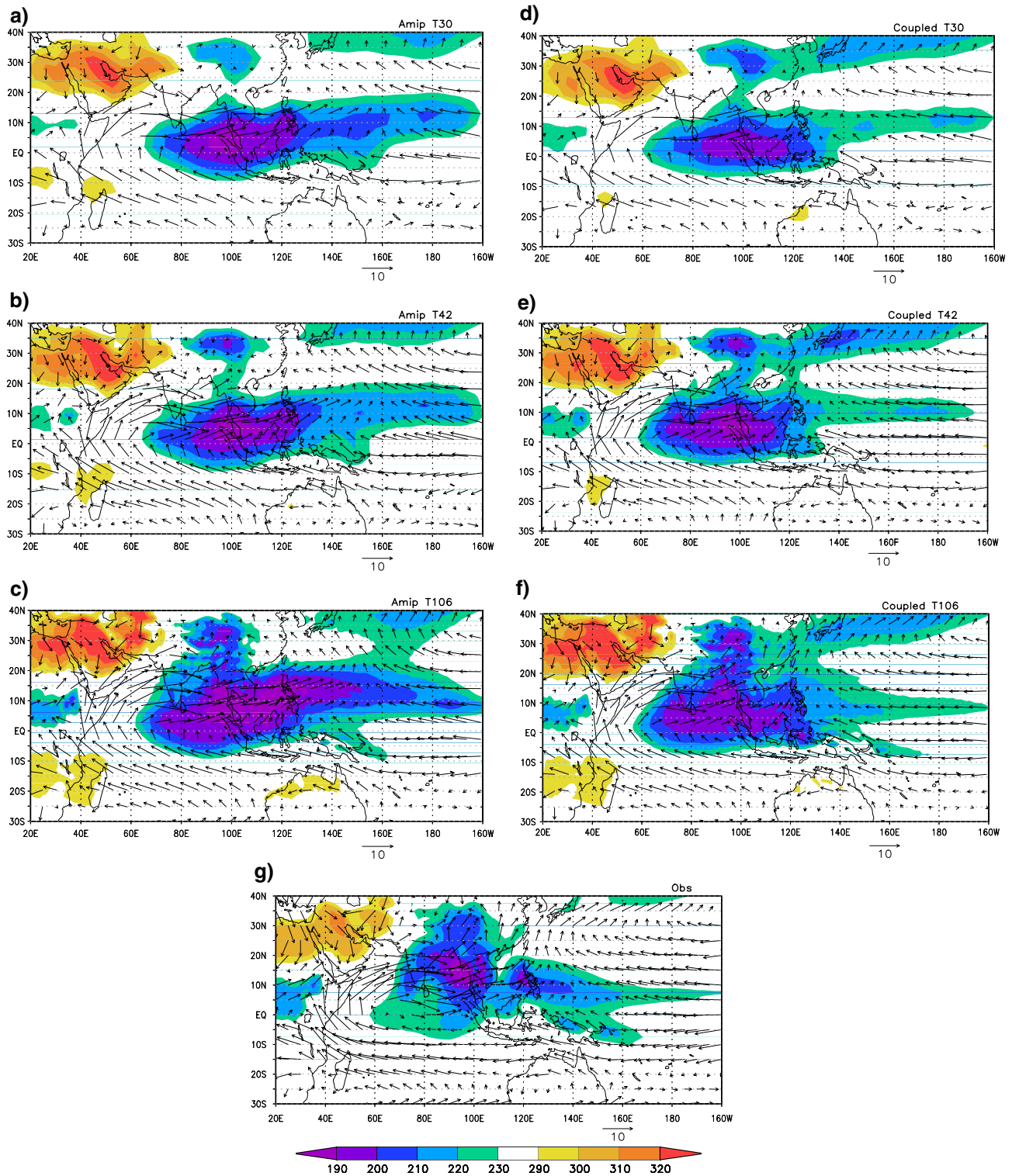
Fig. 1 Mean JJA OLR (W/m²) and surface wind vectors (m/s) for the Echam4 AMIP-type experiments (**a–c**) and the SINTEX coupled model experiments (**d–f**) at three different resolutions (T30, T42 and T106), and for the observations (**g**). OLR data are from NOAA dataset and winds from ERA40 reanalysis
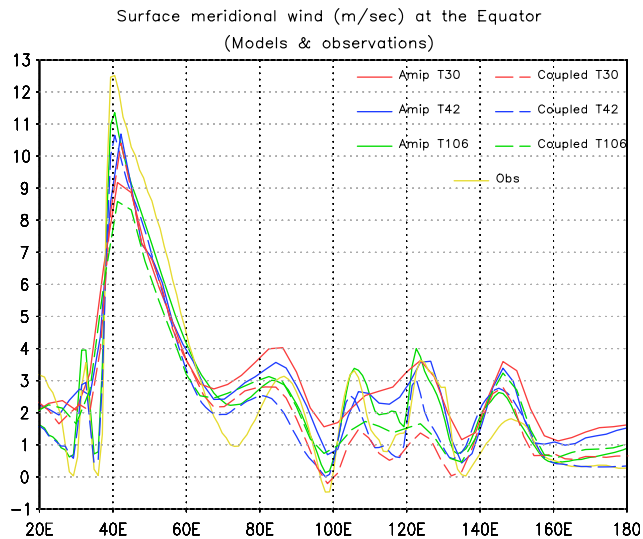
Fig. 2 Mean JJA Equatorial meridional lower tropospheric wind (m/s) for the Echam4 AMIP-type experiments (*solid lines*) and the SINTEX coupled model experiments (*dashed lines*) at three different horizontal resolutions (T30 red, T42 blue and T106 green) and for the ERA40 reanalysis (*yellow solid line*)

observed, producing enhanced convection in that area. The lack of convection over the Bay of Bengal remains a major deficiency in the simulation of the Asian summer monsoon, even at T106 resolution. The main differences between the coupled and the AMIP-type experiments results are around the Philippines, where the coupled model has higher OLR, suggesting the simulation of lower than observed precipitation in that area.

The summer mean precipitation for the Asian monsoon region is represented in Fig. 3. The low resolution experiments results (Fig. 3a, d) show a lack of precipitation all over the Indian area, with the maxima located in the area from 80–100°E and 5°S–20°N. A bias of the precipitation fields for the atmosphere-only model, at all resolutions, is the strong rainfall located in the Western Equatorial Indian Ocean, induced by the strong meridional flow in that area (Fig. 3a–c). In the coupled model experiments this bias is reduced, as well as the meridional wind component. It is interesting to note that as the resolution increases the bias is further diminished. Some aspects of the Indian summer monsoon in terms of precipitation are well captured with an higher resolution model (Fig. 3c, f), even if some convective centres remain located at unrealistic positions. The four main centres of convection of the ISM, that are the Western Ghats, the Bay of Bengal, the Ganges plain and the Equatorial Eastern Indian Ocean, are better captured with the higher resolution model experiments, particularly the understimation of

the Western Ghats and of the Bay of Bengal and the overstimation of the Equatorial Eastern Indian Ocean rainfall are less severe. Over South East Asia the precipitation pattern is better represented at lower resolution for both the AMIP-type and the coupled model experiments results. Around Philippines the precipitation is largely overestimated in the AMIP-type experiments (Fig. 3a–c) and largely underestimated in the coupled model experiments (Fig. 3d–f). Another bias of the coupled model experiments is the double ITCZ over the Western Equatorial Pacific (Fig. 3d–f), typical of other coupled models without flux adjustment (Meehl et al. 2001). This bias is independent from the resolution, suggesting its main dependence on the convective scheme used; these results are confirmed by other coupled models (e.g., Kobayashi and Sugi 2004).

The mean ISM rainfall as simulated by the SINTEX coupled model with the atmospheric component at T30 resolution has been analyzed by Terray et al. (2005). They emphasized that the model was not able to reproduce the heavy rainfall along the western coasts of India and had a bad representation of the distribution of precipitation in the Indian Ocean and the Arabian sea. With an higher resolution atmospheric model component the SINTEX coupled model experiment is able to simulate the abundant precipitation along the Western Ghats (Fig. 3f). The abundant simulated precipitation over the Western Indian Ocean, typical of Echam4, decreases and some rainfall peaks appear nearby the Bay of Bengal even if they are not well localized.

The monthly evolution of precipitation averaged over the main convective areas previously discussed is shown in Fig. 4. The extended indian monsoon rainfall (EIMR) region, introduced by Goswami et al. (1999) includes the Indian subcontinent, the Bay of Bengal and part of the Indian Ocean. Rainfall averaged in the EIMR area (Fig. 4a) is realistically simulated, mainly in terms of starting and ending phase, while the intensity is lower than observed. It is interesting to note that the ending phase is better captured in time and intensity by the T106 model experiments (Fig. 4a, green lines). In the Indian subcontinent (Fig. 4b) the amount of simulated precipitation is slightly underestimated, even if the main peak in July is well captured by the AMIP-type experiments (solid lines) and by the T30 coupled model experiment (red dashed line). The Bay of Bengal seems to be the main cause for the underestimation of the ISM rainfall (Fig. 4c). In the Western Pacific Ocean area (Fig. 4d), the precipitation simulated by the AMIP-type experiments (solid lines) are much stronger than observed (yellow solid line),
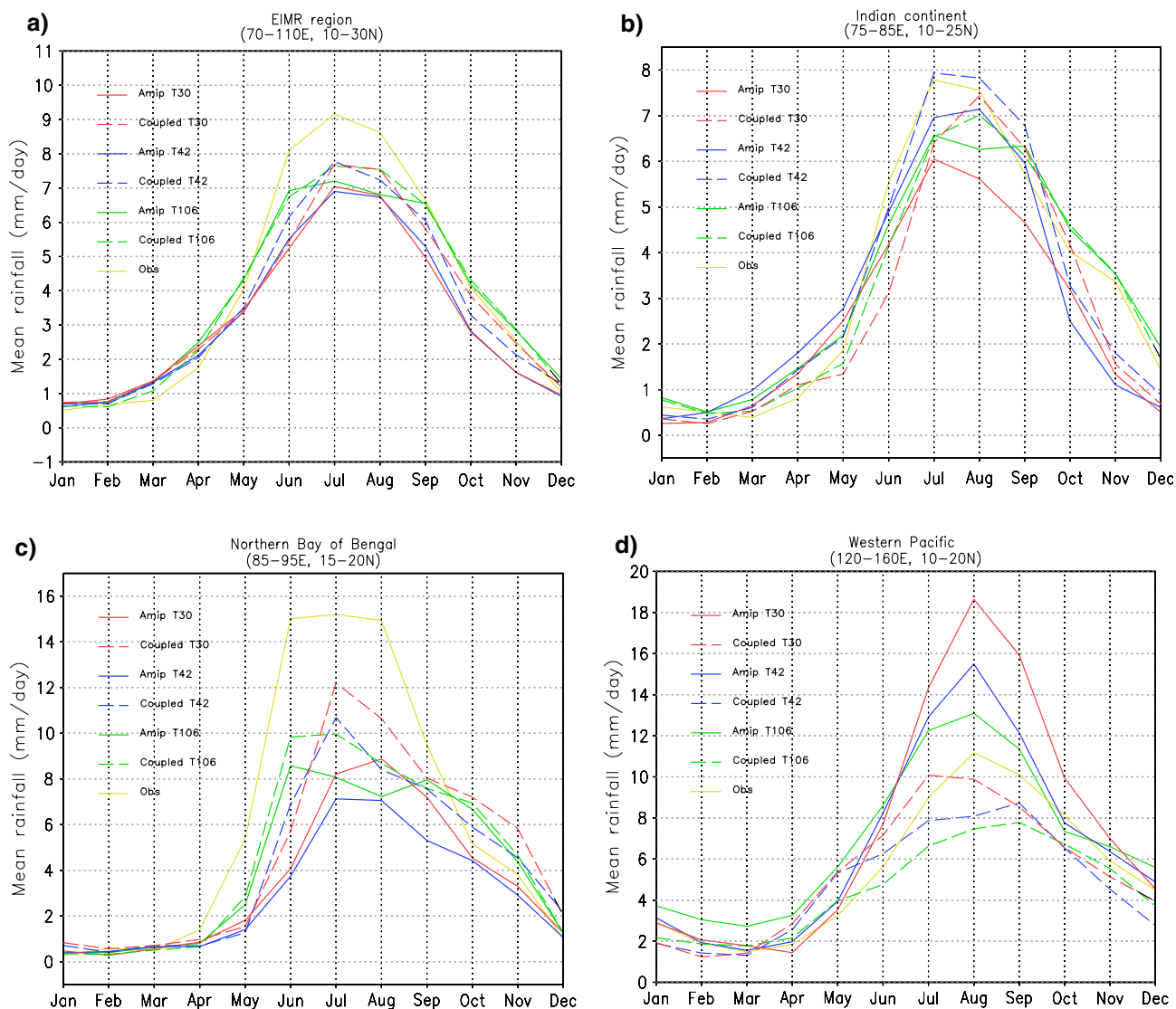
Total precipitation (mm/day)
(Models & observations)
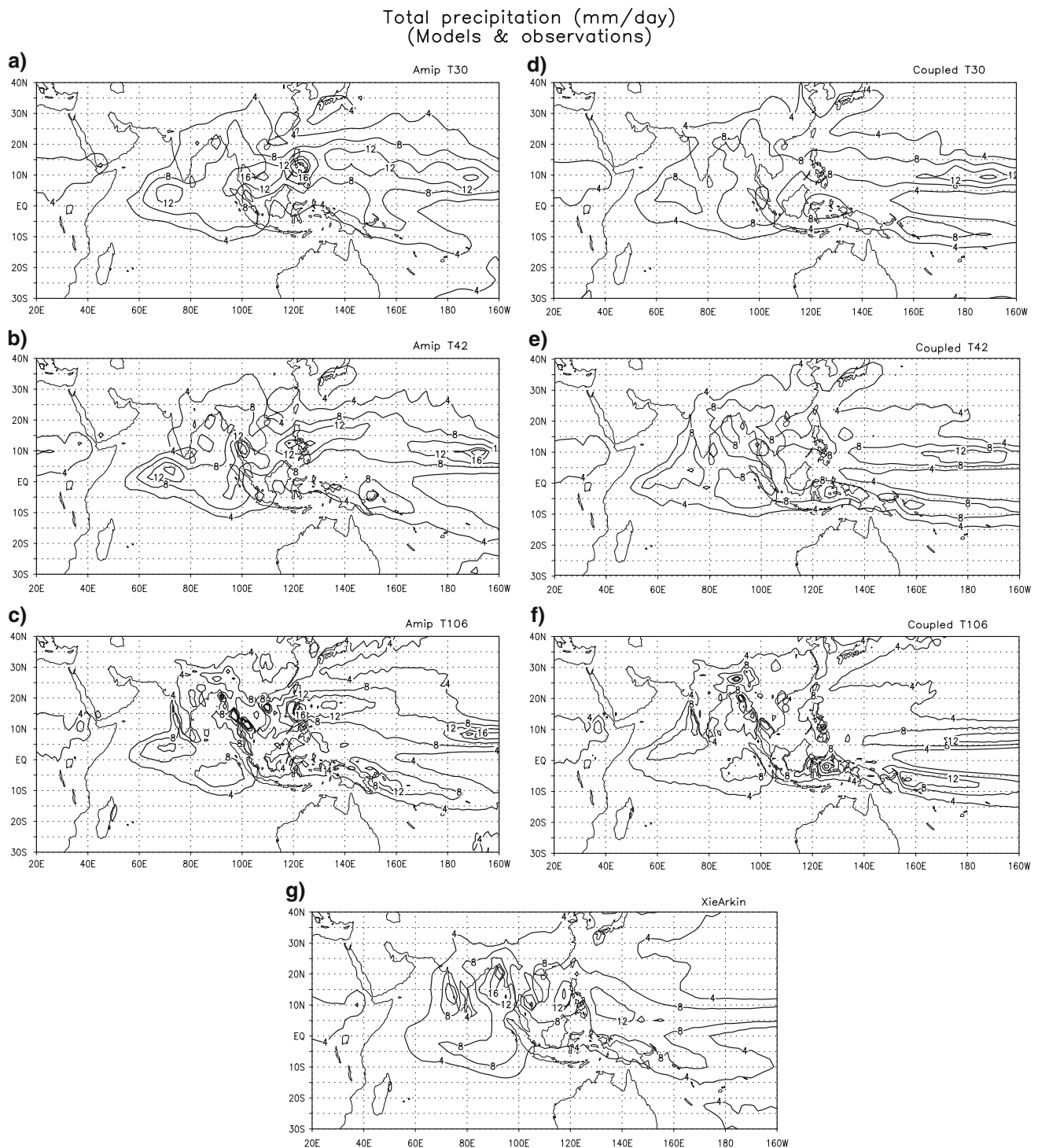
Fig. 3 Mean JJA total precipitation (mm/day) for the Echam4 AMIP-type experiments (**a–c**) and the SINTEX coupled model experiments (**d–f**) at three different horizontal resolutions (T30, T42 and T106) and for the CMAP dataset (**g**). Contour intervals are 4, 8, 12, 16, 18 mm/day

and in the higher resolution experiments they are also anticipated (green solid line). In the Western Pacific Ocean region the rainfall simulated by the coupled model is less than observed (Fig. 4d, dashed lines), it starts in April and from August it decreases rapidly.

4 Possible effects of an interactive ocean

An important forcing for the ASM seems to be the SST in the Tropical Indian Ocean (Shukla 1987; Rao and Goswami 1988; Clark et al. 2000). Indeed, the rela-

Fig. 4 Mean seasonal precipitation averaged in the EIMR region (**a**), in the Indian subcontinent (**b**), in the Northern Bay of Bengal (**c**) and in the Western Pacific area (**d**) for the Echam4 AMIP-type (*solid lines*) and coupled model experiments (*dashed lines*) at three different horizontal resolutions (*T30 blue*, *T42 red*, *T106 green*) and for the CMAP dataset (*yellow solid line*). The averaged areas are specified in *brackets*

tionship between SST in the Tropical Pacific Ocean and the ISM is well recognized (e.g., Webster and Yang 1992; Ju and Slingo 1995; Soman and Slingo 1997; Kinter et al. 2002). Figure 5a shows the mean summer SST observed. In the northern tropical Indian Ocean, summer SST warms up, except in the western part of the basin near the coast of Somalia, where cold water from the below upwells producing a strong gradient. In the coupled model, SST in the Tropical Indian Ocean is warmer than observed, particularly north of the Equator (Fig. 5b–d). For instance, in the northwestern Indian Ocean SST in the coupled model experiments is 1–1.5°C warmer than the HadISST values, and the upwelling region in the western part of the basin is not

simulated. In the Equatorial Pacific Ocean the cold tongue regime simulated by the model extends too westward (Gualdi et al. 2003; Guilyardi et al. 2003). This bias may be responsible for a worse simulation of the connection between ENSO and the monsoon (Terray et al. 2005). In the North Eastern Tropical Pacific Ocean the simulated SST is colder than observed, especially at lower resolutions (Fig. 5b, c), and this may be associated to the weaker representation of the surface winds and precipitation in the western north Pacific monsoon region.

The impact of air–sea coupling processes in the simulation of the Asian summer monsoon has been analyzed by Fu et al. (2002). They argued that the

Fig. 5 Mean JJA SST (°C) from the HadISST dataset (**a**), used to force the atmospheric model. The observed field has been subtracted from the coupled model results at T30, T42 and T106 resolution (**b–d**, respectively). Contour intervals are − 4, − 2, − 1, − 0.5, 0.5, 1, 2, 4, 6°C. The *thicker line* corresponds to the zero contour
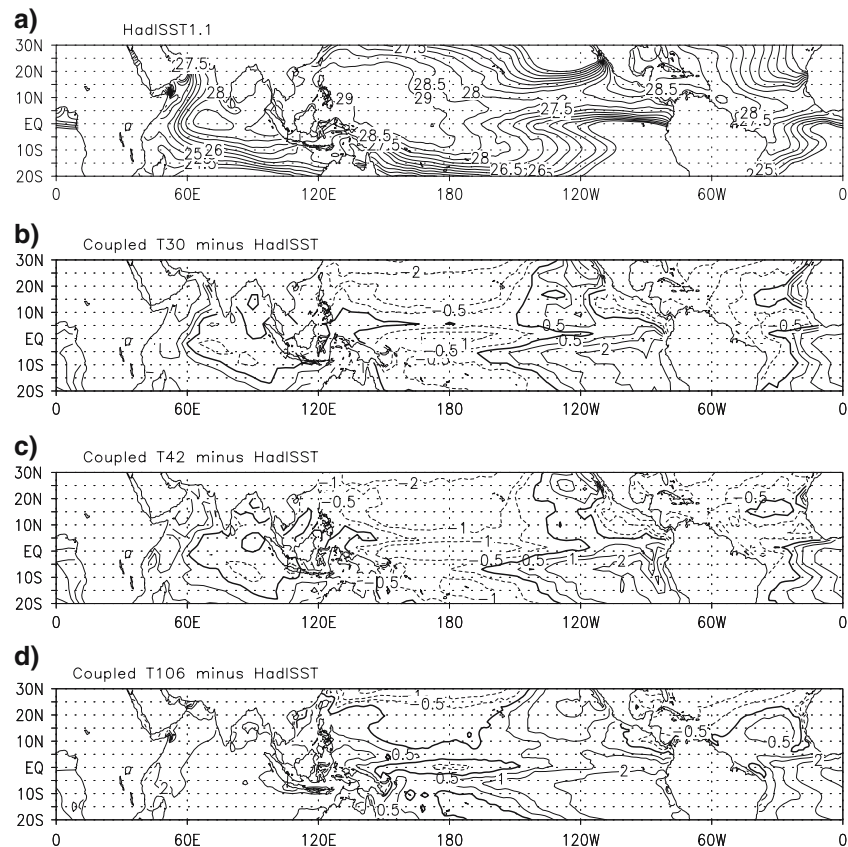
coupling was able to overcome some deficiencies of the atmospheric model alone. In particular, the cold bias they found in the coupled model SST was able to favour interaction with SST, fluxes and winds, producing results more similar to the observations.

The analysis of the previous section has shown that in some regions (i.e. Western Ghats, Bay of Bengal, Western Equatorial Indian Ocean and Indonesia) the coupled model simulates more precipitation with respect to the atmospheric model alone, whereas in others (i.e. Eastern Equatorial Indian Ocean and northwestern tropical Pacific Ocean) it simulates less precipitation. To analyze with more details the effective role of the SST, a new set of experiments has been built with the atmospheric model forced by SST obtained from the coupled model simulations. The experiments have been performed for each horizontal resolution and integrated for 10 years.

The Echam4 model when forced by SST with a warm bias in the Indian Ocean and with a cold bias in the North Western Pacific Ocean simulates a South Asian summer monsoon with more rainfall in the Bay of Bengal and in the Indian subcontinent, and with less rainfall in the Eastern Equatorial Pacific Ocean and in the North Western Pacific Ocean. The south-westerly

flow in the Indian Ocean is weaker in the new experiments (Fig. 6). In particular, both the zonal and the meridional components are weaker in the Equatorial band and just south of it, and they are stronger north of it in correspondence of the Indian subcontinent and of South East Asia.

The differences between the coupled model simulations and the results from the forced experiments are almost weak suggesting the hypothesis that in the coupled model the bias in the SST is the dominant influence

5 Interannual variability: monsoon indices analysis

The interannual variability of precipitation may be analyzed by means of an EOF analysis applied to the summer mean precipitation. This analysis has been made for the AMIP-type experiments and for the coupled model to evidence which is the influence of prescribed or interactive SST on the monsoon variability. The EOF has been applied to the area 20°S–40°N for all the longitudes, as Navarra et al. (1999) shown that it is the best area to capture the interannual variability of the tropical regions. Precipitation fields
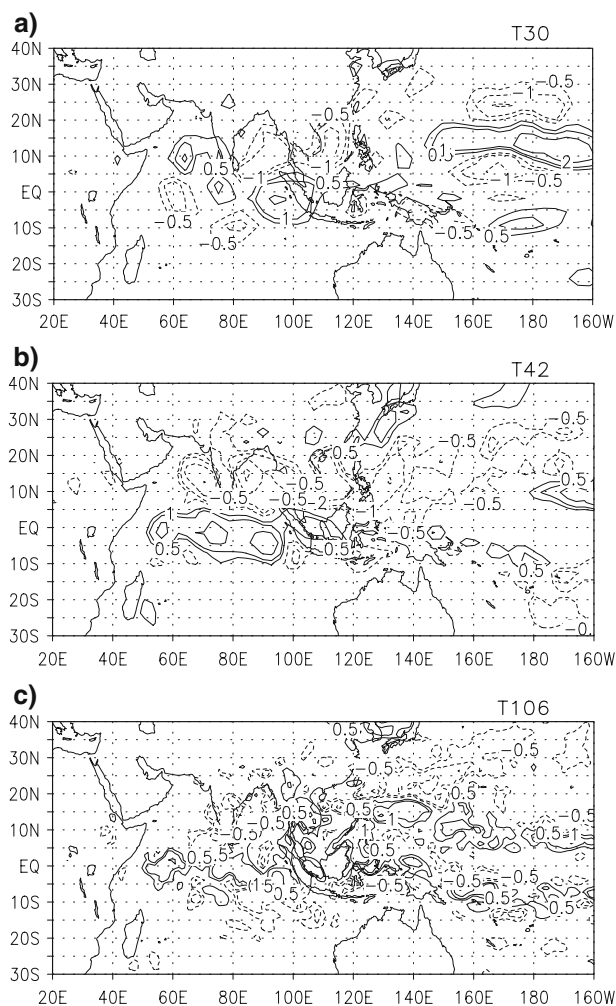
Fig. 6 Mean JJA total precipitation differences between coupled model experiments and atmospheric model with SST forced from the coupled model. Contour interval is 0.5 mm/day

have been averaged from June to August. In the ENSO-monsoon region, the areas with the higher variability are localized in the Pacific Ocean, south of the Equator along the whole basin, and north of the Equator in the North East near the coast of America, and in an area which includes the Maritime Continents, the South China sea, the south-eastern Tropical Indian Ocean and part of the Indian subcontinent (Fig. 7g). The areas identified are of opposite sign, suggesting an inverse connection between them. In the observations the percentage of variance explained by this mode is 13%. The dominant mode of variability of the summer precipitation just described is partially simulated by the models. The negative pattern in the Pacific Ocean is captured by both coupled and atmospheric model, even if in the coupled model it extends westward reaching the Maritime Continents region, possibly as a consequence of the bias of the coupled model which

simulates a cold tongue regime which extends too westward (Gualdi et al. 2003; Guilyardi et al. 2003). On the other hand the positive pattern is weaker at high resolution. The weakness of the EOF pattern is present even in the coupled model experiments, suggesting its dependence on the horizontal resolution of the atmospheric component rather than to the presence or absence of an interactive ocean. In the Maritime Continents region the sign is unrealistically reversed with respect to India in the AMIP-type experiments.

Usually, strong and weak monsoon years are distinguished with indices based on precipitation and wind fields. The simulation of the interannual variability of the monsoon rainfall widely differs from one model to another (Sperber and Palmer 1996), and this suggests that some regional aspects of the circulation strongly depend on the resolutions and on the physical parameterizations of the models. In the literature a large number of circulation-based indices has been introduced with the main aim to study the different aspects of the monsoon. Furthermore, when dealing with the general circulation models, the indices have to be selected with some consideration of the systematic errors of each model.

The dynamical monsoon index (DMI) is a well-known circulation-based index. It was defined by Webster and Yang (1992) as the mean JJA zonal wind shear (u_{850} – u_{200}) on the area 40°–110°E, Equator – 20°N, and it has been used in many studies (e.g., Ju and Slingo 1995; Li and Yanai 1996; Lau et al. 2000) to represent the broad scale features of the Asian monsoon. The DMI simulated by the Echam4 model is significantly correlated (Table 1) with the observations at all resolutions. The increase of the resolution does not change the significance of the correlation with the observations, this result may suggest that SST has a stronger impact on this variability than the horizontal resolution has. As the DMI is considered a large-scale dynamic index, we should assume that our model successfully simulates these global features. Besides, as the DMI have been recognized to be related to the Walker circulation over the Indian Ocean region (Goswami et al. 1999), it may be argued that the model can simulate also this component of the monsoon circulation.

Composite maps of strong minus weak years according to DMI are computed to investigate the spatial structure of the monsoon variability. A significance test based on the bootstrap procedure has been applied to the composite maps. Values significant at 95% are shaded in the pictures. In the observations (Fig. 8g), a strong monsoon is characterized by higher
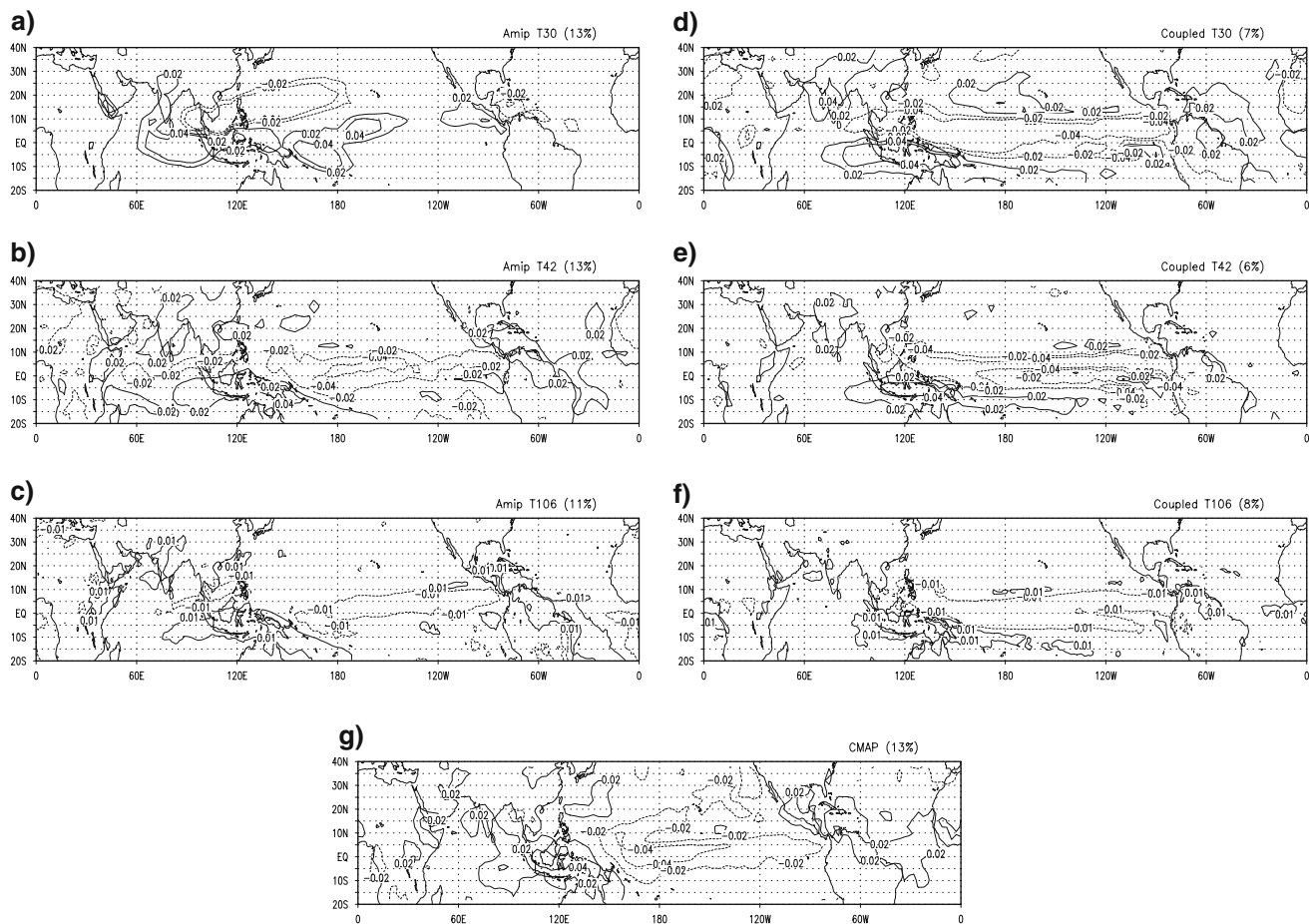
Fig. 7 First EOF for the JJA mean precipitation (mm/day) for the AMIP-type experiments (**a–c**), for the coupled model experiments (**d–f**) and for the observations (**g**)

Table 1 Linear correlation coefficients of DMI and MHI indices as computed from the ERA40 reanalysis wind fields and the Echam4 AMIP-type experiments at three different horizontal resolutions (T30, T42 and T106)

|	T30	T42	T106
DMI	0.53*	0.49*	0.47*
MHI		0.40*	0.20

Asterisks indicate values significant above 99%

than normal precipitation over India, in the Bay of Bengal and in the North Western Pacific Ocean near Philippines, and by lower than normal precipitation in the Equatorial Pacific Ocean and in the Equatorial Indian Ocean.

In the AMIP-type experiments, strong monsoon years are characterized by intense precipitation over India (Fig. 8b, c), specifically in the Bay of Bengal and in the Western Ghats. The lower resolution experiment (Fig. 8a) is not able to capture the variability along the Western Ghats. In the coupled model experiments (Fig. 8d–f) the spatial distribution of the composites of

rainfall anomalies over India is quite similar to the AMIP-type experiments results. In particular, a strong monsoon year is associated with strong precipitation over the Bay of Bengal and in the Western Ghats, and this pattern is simulated even at low resolution. It is interesting to note that intense precipitation over India is associated with intense precipitation over the Philippines and less than usual precipitation over the Equatorial Indian Ocean, over Indonesia and in the Eastern Equatorial Pacific Ocean, as observed.

The intensification of the precipitation over the Bay of Bengal is associated to an intensification of the low-level westerly flow towards India and in the Bay of Bengal (Fig. 9g). The increase of precipitation in the North Western Pacific Ocean is associated to a cyclonic flow (Fig. 9g) which is simulated better at higher resolution for both forced and coupled model experiments. The intensity of the low-level westerly flow towards India is realistically captured by the models (Fig. 9). There are some biases over the Bay of Bengal, especially in the coupled model at low resolutions
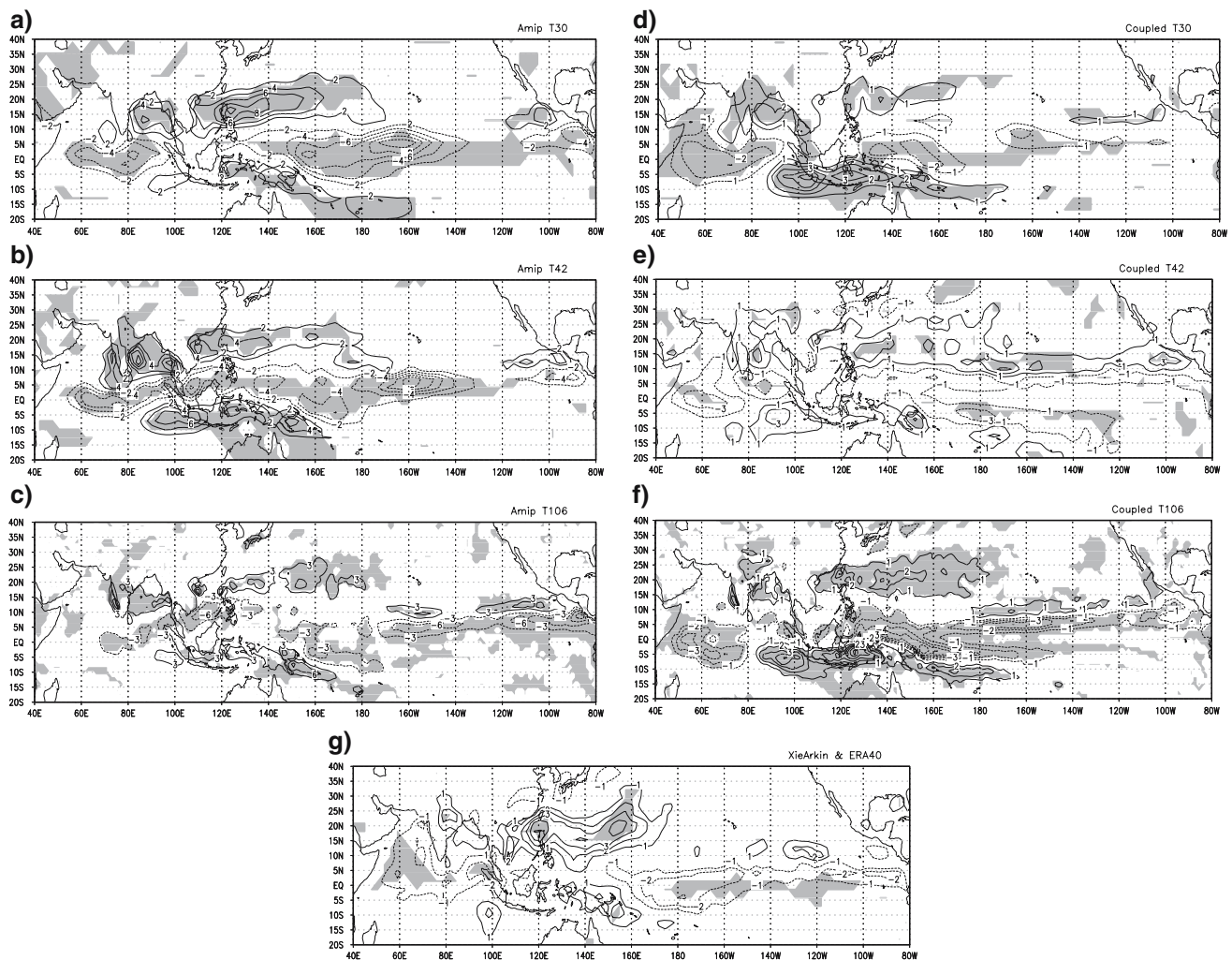
Fig. 8 Composite maps of strong minus weak JJA precipitation anomalies (mm/day) according to DMI for the Echam4 AMIP-type (**a–c**), coupled model experiments (**d–f**), and the ERA40 reanalysis (**g**). *Shaded values* are significant at 95%

(Fig. 9d, e), where the westerly flow is weaker and it is deflected southward. Furthermore, in the coupled model, mainly at low resolutions (Fig. 9d, e), the cyclonic flow in the North Western Pacific Ocean is not well simulated.

Another important monsoon index is the monsoon Hadley index (MHI) that was defined by Goswami et al. (1999) as the mean summer meridional wind shear (v_{850} - v_{200}) averaged in the area 70–110°E, 10–30°N. It was introduced to represent the strength of the ISM circulation. As the DMI is related to the Walker circulation, the MHI has been introduced as related to the Hadley circulation, both of them being important for the evolution of the monsoon.

The MHI simulated by the Echam4 model is positively correlated with the observations, but the correlation is significant only for the T42 resolution experiment (Table 1), this implies that the horizontal

resolution does not help to reduce the systematic errors associated to the local Hadley circulation. The analysis of the linear correlation between the simulated MHI and that from reanalysis suggests that the 1980s have a better correlations with the observations for all the resolutions, the main deficiencies are found in the last decade and in the 1970s (not shown).

Strong monsoon years according to MHI (Fig. 10g) have higher precipitation over India and in the southwestern Indian Ocean, and negative anomalies in the South Eastern Indian Ocean and along the Equatorial Pacific Ocean. In the AMIP experiments case (Fig. 10a–c) positive anomalies over India are associated with negative anomalies over the West Pacific Ocean and positive anomalies over the south eastern Indian Ocean. The negative relation with the Eastern Equatorial Pacific Ocean is prominent at T106 resolution (figure 10c). In the coupled model experiments,
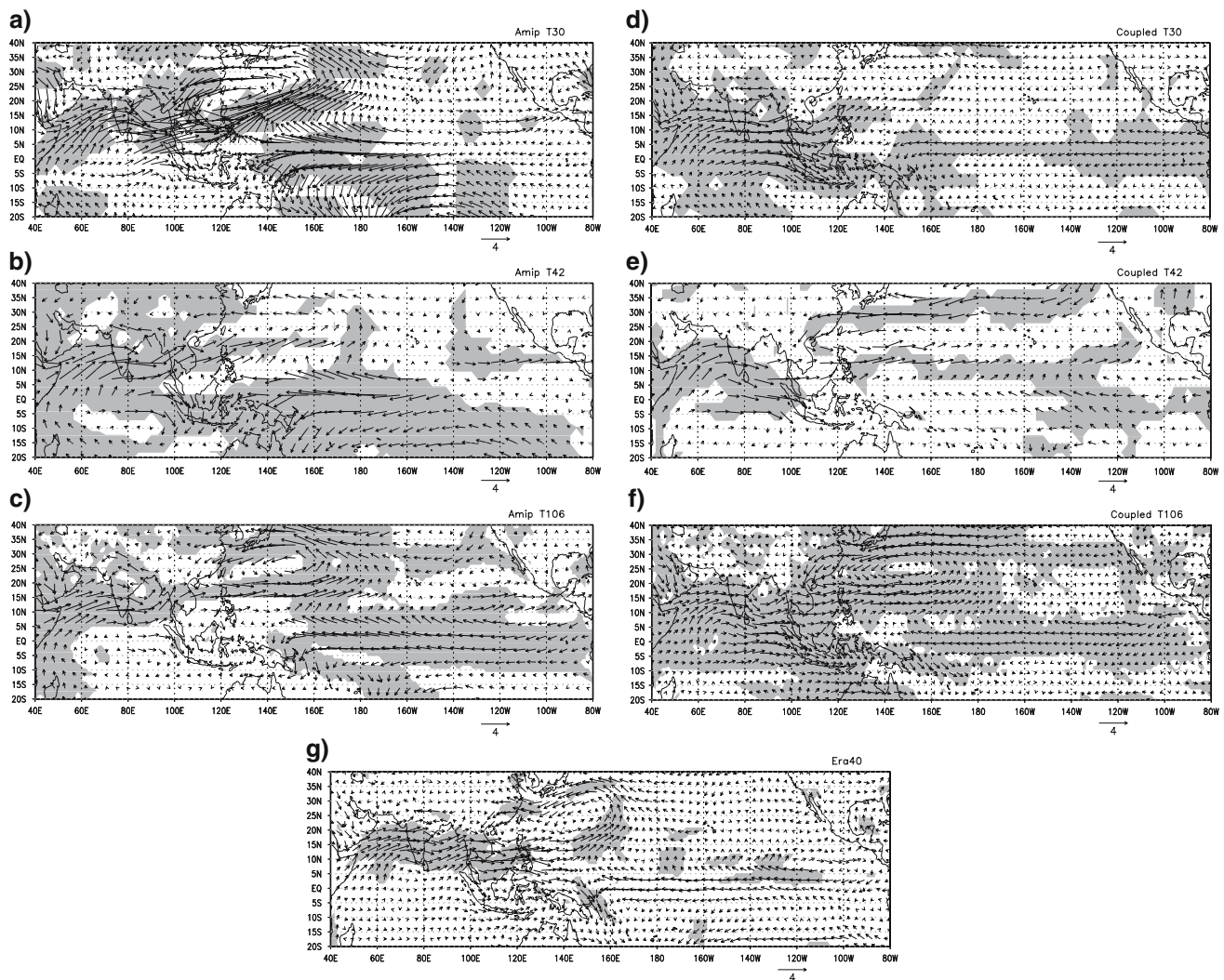
Fig. 9 Composite maps of strong minus weak JJA wind anomalies (m/s) at 850 mb according to DMI for the Echam4 AMIP-type (**a–c**), coupled model experiments (**d–f**), and the ERA40 reanalysis (**g**). *Shaded values* are significant at 95%

negative anomalies over the Equatorial Pacific Ocean are present at all resolutions (Fig. 10d–f). Positive anomalies in the Indian subcontinent are associated to positive anomalies in the western Equatorial Indian Ocean, as observed. The negative relationship between India and south eastern Equatorial Indian Ocean is not captured by the coupled model. In the DMI composite precipitation anomalies at T106 resolution are weaker than at lower resolution, while in the MHI case the values are comparable. If the DMI (MHI) links the monsoon variability to the Walker (Hadley) circulation we may argue that at higher resolution the Echam4 model fails the simulation of the Walker circulation affecting the tropical variability, including the monsoon.

The main differences in the composites of the winds at low levels between MHI and DMI are over the Bay of Bengal, where in the first case the intensification of

the flow is towards north while in the second case it is mainly westward, and in correspondence of South Eastern China, where in the second case there is a strong westerly flow that reaches the Philippines Islands (not shown). Those features are not captured by the models. Both the coupled and the atmospheric models have a strong easterly flow in the region from 100°E and 140°E that is unrealistic. It is possibly a shortcoming in the models to represent realistically the Hadley circulation component in the ENSO-monsoon region (not shown).

6 ENSO-monsoon connection: the 1976 climate shift

The Asian monsoon and ENSO are interactive systems (Webster and Yang 1992), each of them being able to influence and to be influenced by the other. The
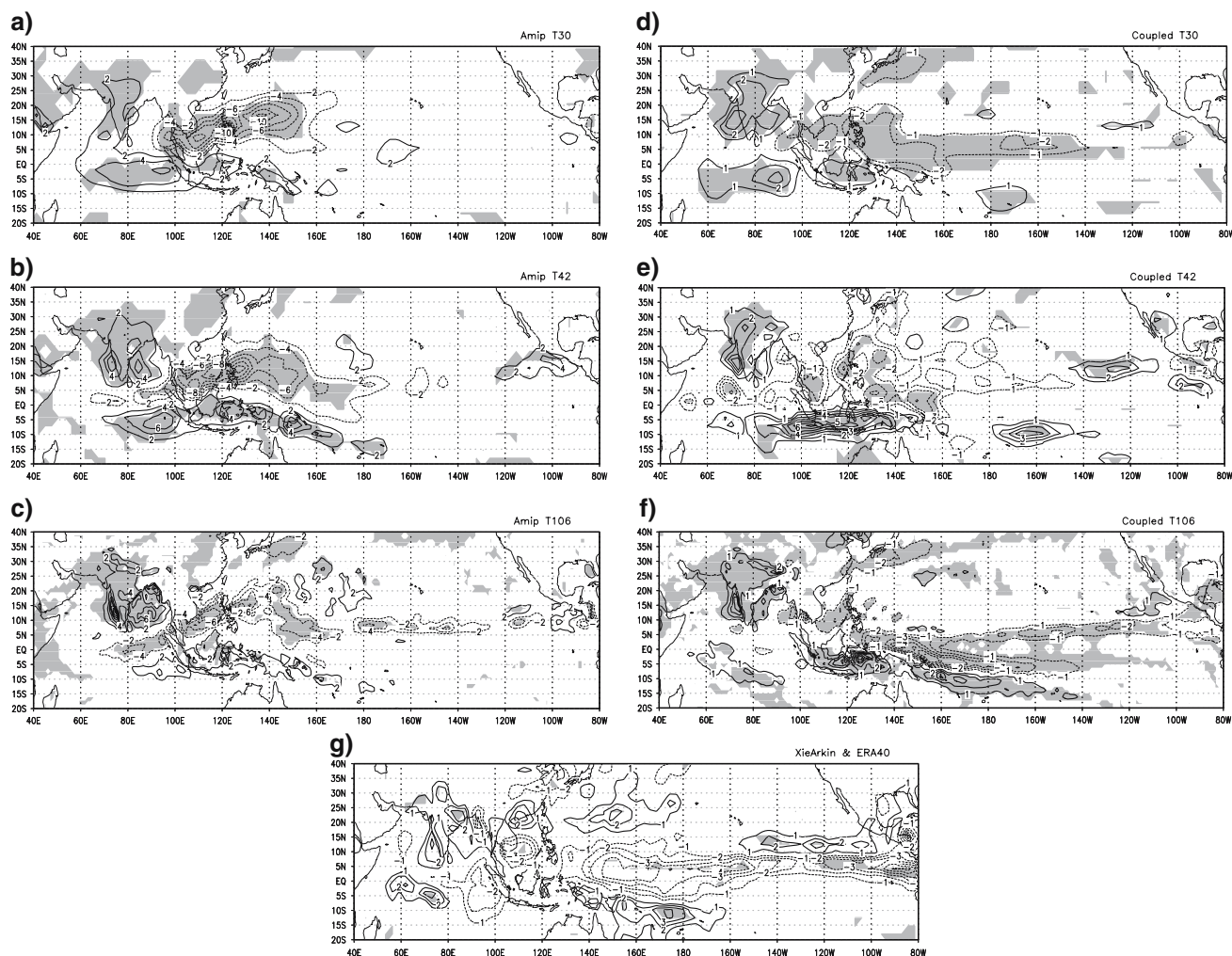
Fig. 10 Composite maps of strong minus weak JJA precipitation anomalies (mm/day) according to MHI for the Echam4 AMIP-type (**a–c**), for the coupled model experiments (**d–f**) and for the observations (**g**). *Shaded values* are significant at 95%

physical connections through which the South Asian monsoon influences ENSO should be investigated with an analysis of the indices that measure the monsoon. Some studies (e.g., Ju and Slingo 1995; Webster et al. 1998) have shown that the Indian monsoon and ENSO are inversely correlated. The DMI previously discussed is considered a good index to represent the dynamical aspect of the Asian monsoon and is choosen here to analyze the connection with ENSO. The DMI is significantly correlated with the NINO3 index, while the MHI, in the models, has a weaker correlation (not shown). This behaviour indicates that ENSO influences the monsoon mainly through the Walker circulation, whereas the local Hadley cell is less affected.

There are evidences that in last decades the connection between ENSO and the monsoon has decreased (Kumar et al. 1999b). Changes in this connection may be associated to changes in the Tropical North Pacific Ocean climate and in the low-level

circulation with centres in the South China sea and Philippines Islands (Kinter et al. 2002).

The maps of the correlation coefficients of DMI with global SSTs have been computed for the AMIP-type experiments in two different periods: before 1976 (from 1956 to 1976) and after 1976 (from 1977 to 1999) to investigate the effects of those changes in the atmospheric model. SST is a fundamental and important Oceanic indicator of the ENSO process (Kinter et al. 2002); furthermore, JJA is the season where the connection is established and strong (Kumar et al. 1999a). Those kind of maps may give information also on the influence of the monsoon on ENSO itself. The correlation field (Fig. 11h) is characterized by the horseshoe pattern over the Pacific Ocean (as defined by Miyakoda et al. 1999). To the west the horseshoe pattern is surrounded by a region of opposite sign and it is connected with other correlations over the Indian Ocean. In the AMIP-type experiments (Fig. 11a–c) the

pattern described is realistically captured at all resolutions. It is noteworthy that DMI and Eastern Equatorial Pacific SSTs have a strong negative correlation. This result supports the idea that the DMI may represent the large-scale circulation changes over the Indian Ocean associated with ENSO (Goswami et al. 1999).

From the picture it is evident that the correlation has decreased after 1976 (Fig. 11e—h). The decrease of the correlation in the Eastern Equatorial Pacific Ocean is associated with a decrease of the negative correlation in the Indian Ocean and with an increase of the positive correlation in the Western Tropical Pacific Ocean.

The analysis of the precipitation before and after 1976 in the model results reveals that in correspon-dence of a weakening of the relationship between ASM and ENSO there is a weakening (down to 3–4 mm/day) of the rainfall amount in the Indian sub-continent and in the Bay of Bengal, and an intensifi-cation (up to 6–8 mm/day) of the precipitation in the Western North Pacific Ocean (not shown). The same behavior is simulated at all the resolutions considered.

7 Discussions and conclusions

The ASM is simulated by the Echam4 model in a realistic way, at least in terms of circulation and pre-cipitation features. In particular, the low level westerly flow, that is the dominant manifestation of the Asian summer monsoon, is well captured by the model at all
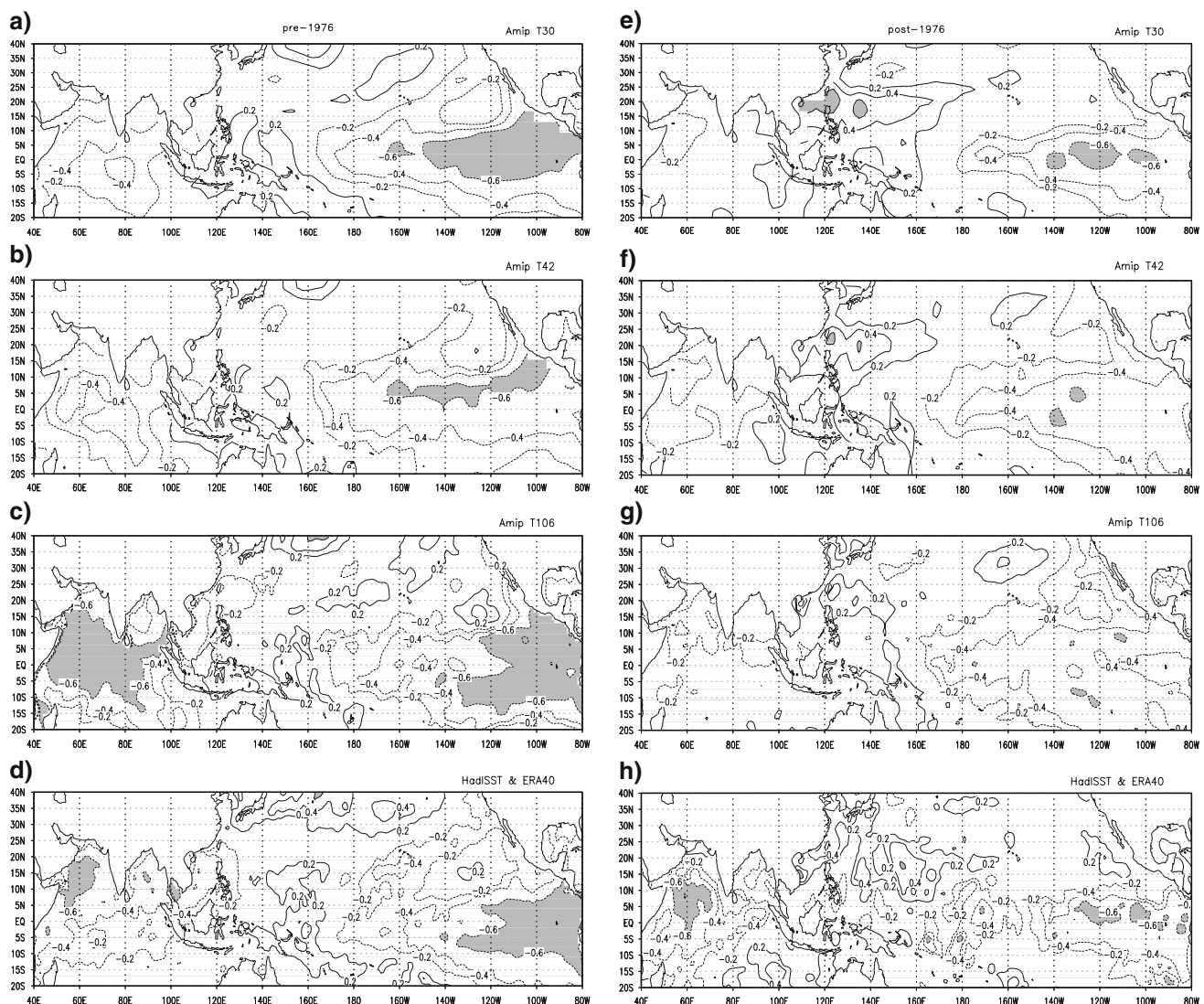
Fig. 11 Correlation maps of JJA mean SST and DMI for the Echam4 AMIP-type experiments and the reanalysis. *Left panels* for the period before 1976 and *right panels* for the period after 1976. *Shaded values* are lower than − 0.6 and higher than 0.6

resolutions, and the precipitation is realistically simulated either in space distribution and intensity. The precipitation around the Equatorial zone are stronger than observed, a common problem for many atmospheric models. The major deficiencies of the model are the lack of precipitation over the Bay of Bengal and a meridional wind at the Equator stronger than observed. A probable explanation for the lack of precipitation in the Bay of Bengal is the deficiency of the model to simulate well the surface winds from the Eastern African Highlands preventing the migration of rainfall into the Indian Ocean and the Indian subcontinent. The increase of the horizontal resolution improves the simulation of some regional aspects of the monsoon, for example the higher resolution experiment reproduce the precipitation on the Western Ghats, that is completely absent at lower resolution, mainly because of an improvement in the orography. However, higher resolution can not represent the entire solution for the systematic errors of the models.

The interaction between atmosphere and ocean is important for a good representation of the Asian monsoon. Anyway, as shown in Sect. 3, the SINTEX coupled model tends to overestimate the SST in the Indian Ocean. Furthermore, the SST gradient in the western part of the basin near Somalia is weak in the coupled model: a consequence is the weakening of the surface winds from the Indian Ocean towards India. Precipitation and surface winds as simulated by the coupled model are realistic, somehow they are better than in the forced model, but somehow they are worse. Over India and in the Equatorial Indian Ocean the simulated precipitation in the coupled model is slightly reduced with respect to the atmospheric model and more similar to the observations, but around Philippines it is largely underestimated than in the atmospheric model forced with prescribed SST and in the observations. The set of experiments performed with the atmospheric model forced with SST from the coupled model helped to distinguish in some way the importance of an interactive Ocean for the simulation of the Asian summer monsoon. The differences between the results of the coupled model experiments and the results of the new forced experiments are small (lower than 2 mm/day). When the atmospheric model is forced with SST computed from the coupled model, it tends to simulate more precipitation over the Indian subcontinent and in the Western Tropical Pacific Ocean, but less precipitation over Indonesia and along the Equatorial Indian Ocean. The systematic error in the SST, presumably in the Indian Ocean, seems to be the main reason for the difference between the AMIP experiment and the coupled model.

The Echam4 model is able to realistically simulate the interannual variability of the Asian summer monsoon. Winds field are better simulated than precipitation in the model, as a consequence circulation-based indices are better correlated with observations. The indices used for the analysis, DMI and MHI, are both dynamical indices. The DMI has been introduced to study the variability of the large-scale monsoon. In our models it represents the variability of the Indian summer monsoon as well, and as it is significantly correlated with the reanalysis it has been used to study the spatial variability of precipitation and wind fields in correspondence of strong and weak monsoon. The results from the coupled model experiments are encouraging of the ability of that model to reproduce the ASM and its dynamics. The other index used, the MHI, has been introduced as a representation of the variability of the ISM associated to the Hadley circulation. The correlation between the index computed from the AMIP-type experiments wind fields and that from ERA40 reanalysis is not significant and the resolution does not help to solve this issue.

The analysis of the interannual variability of the monsoon has been extended to the coupled model results, with the main aim to analyze the differences among the models. As a first step an EOF analysis has been computed for precipitation fields. The main result of this analysis is that the intensity of the variability is reduced at high resolution. In both forced and coupled model the areas of higher precipitation variability are localized over Indonesia and in the Eastern Equatorial Indian Ocean. The positive anomaly in the Eastern Equatorial Indian Ocean is linked with an anomaly of the same sign over India.

Composite analysis of precipitation and winds according to DMI and MHI are then used to analyze the spatial difference on the sequence of strong and weak monsoon years in forced and coupled model. The DMI is used to follow the dependence of the monsoon circulation on the Walker circulation, while the MHI is chosen to investigate the relevance of the Hadley circulation. Strong monsoon years are characterized by abundant precipitation over India and less than normal precipitation in the Indian Ocean and along the Equatorial Pacific Ocean. According to MHI, precipitation are weaker during strong monsoon years in the north western Pacific, differently from the DMI case, mainly as a consequence of a local effect. The main features described are repeated at all resolutions. The main differences between the forced experiments and the coupled model experiments are found in the composites of the wind fields.

The connection between ENSO and the monsoon has been studied as well. In particular, the AMIP-type experiments results have been used to compute the correlation between SST and DMI in summer before and after 1976, following the analysis made by Kinter et al. (2002). As in the observations the relationship between the monsoon and SST in the Eastern Equatorial Pacific Ocean in summer is negative. Interestingly, this connection decreases in recent decades, as shown by previous observational studies (e.g., Kumar et al. 1999b; Kinter et al. 2002).

We may summarize the main conclusions of this work as follows:

- the Echam4 model either coupled or uncoupled is able to simulate the ASM in a realistic way.
- an higher horizontal resolution of the atmospheric model helps to better represents some regional aspects of the precipitation, e.g., in the Western Ghats.
- error compensation in the coupled model seems to reduce some systematic errors in precipitation and wind fields simulation in the Equatorial Indian Ocean.
- the interannual variability in the AMIP-type experiment is realistic, with weak differences among the resolutions, suggesting its stronger connection with the SST representation.
- the atmospheric model is able to capture the negative relationship between monsoon and ENSO as well as the weakening of that connection observed after 1976.

The results shown indicate that the increase in the resolution alone is not able to solve all the errors of the model. However, high resolution seem to be a prerequisite to have a better simulation of the precipitation.

References

Annamalai H, Slingo JM, Sperber KR, Hodges K (1999) The mean evolution and variability of the Asian summer monsoon: comparison of ECMWF and NCEP/NCAR reanalysis. Mon Weather Rev 127:1157–1186

Cherchi A, Navarra A (2003) Reproducibility and predictability of the Asian summer monsoon in the Echam4 GCM. Clim Dyn 20:365–379

Clark CO, Cole JE and Webster PJ (2000) Indian Ocean SST and Indian summer monsoon rainfall: predictive relationships and their decadal variability. J Clim 13:2503–2519

Dümenil L, Bauer HS (1998) The tropical easterly jet in a hierarchy of GCMs and reanalyses. MPI-Report 247:45 pp

Fennessy MJ, Kinter III JL, Kirtman B, Marx L, Nigam S, Schneider E, Shukla J, Straus D, Vernekar A, Xue X, Zhou J (1994) The simulated Indian monsoon: a GCM sensitivity study. J Clim 7:33–43

Fu X, Wang B, Li T (2002) Impacts of air–sea coupling on the simulation of mean Asian summer monsoon in the EC-HAM4 model. Mon Weather Rev 130:2889–2904

Gates WL (1992) AMIP: the atmospheric model intercomparison project. Bull Am Meteorol Soc 73:1962–1970

Goswami BN (1998) Interannual variations of Indian summer monsoon in a GCM: external conditions versus internal feedbacks. J Clim 11:501–521

Goswami BN, Krishnamurthy V, Annamalai H (1999) A broad scale circulation index for the interannual variability of the Indian summer monsoon. Q J R Meteor Soc 125:611–633

Gualdi S, Navarra A, Guilyardi E, Delecluse P (2003) Assessment of the tropical Indo-Pacific climate in the SINTEX CGCM. Ann Geophys 46:1–26

Guilyardi E, Delecluse P, Gualdi S, Navarra A (2003) Mechanisms for ENSO phase change in a coupled GCM. J Clim 16:1141–1158

Hastenrath S (2000) Zonal circulations over the Equatorial Indian Ocean. J Clim 13:2746–2756

Inatsu M, Kimoto M (2005) Difference of boreal summer climate between coupled and atmosphere-only GCMs. SOLA 1:105–108 doi:10.2151/sola.2005-028

Ju J, Slingo J (1995) The Asian summer monsoon and ENSO. Q J R Meteor Soc 121:1133-1168

Kinter III JL, Miyakoda K, Yang S (2002) Recent changes in the connection from the Asian monsoon to ENSO. J Clim 15:1203–1215

Kitoh A, Arakawa O (1999) On overestimation of tropical precipitation by and atmospheric GCM with prescribed SST. Geophys Res Lett 26(19):2965–2968

Kitoh A, Yukimoto S, Noda A (1999) ENSO–monsoon relationship in the MRI Coupled GCM. J Meteorol Soc Jpn 77:1221–1245

Kobayashi C, Sugi M (2004) Impact of horizontal resolution on the simulation of the Asian summer monsoon and tropical cyclones in the JMA global model. Clim Dyn 93:165–176

Kumar KK, Kleeman R, Cane MA, Rajagopalan B (1999a) Epochal changes in Indian monsoon–ENSO precursors. Geophys Res Lett 26(1):75–78

Kumar KK, Rajagopalan B, Cane MA (1999b) On the weakening relationship between the Indian monsoon and ENSO. Science 284:2156–2159

Latif M, Barnett TP (1994) Causes of decadal climate variability over the North Pacific and North America. Science 266:634–637

Lau NC, Nath MJ (2000) Impact of ENSO on the variability of the Asian–Australian monsoons as simulated in GCM experiments. J Clim 13:4287–4309

Lau KM, Kim KM, Yang S (2000) Dynamical and boundary forcing characteristics of regional components of the Asian summer monsoon. J Clim 13:2461–2482

Li C, Yanai M (1996) The onset and interannual variability of the Asian summer monsoon in relation to land–sea thermal contrast. J Clim 9:358–375

Lindzen RS, Nigam S (1987) On the role of sea surface temperature gradients in forcing low-level winds and convergence in the Tropics. J Atmos Sci 44(17):2418–2436

Madec G, Delecluse P, Imbard M, Levy C (1998) OPA version 8.1 Ocean general circulation model reference manual. Technical report LODYC/IPSL Note 11

May W (2003) The Indian summer monsoon and its sensitivity to the mean SSTs: simulations with the ECHAM4 AGCM at T106 horizontal resolution. J Roy Meteorol Soc Jap 81(1):57–83

Meehl GA (1989) The coupled ocean–atmosphere modelling problem in the tropical Pacific and Asian monsoon regions. J Clim 2:1146–1163

Meehl GA, Arblaster JM (1998) The Asian–Australian monsoon and El Niño-Southern Oscillation in the NCAR climate system model. J Clim 11:1356–1385

Meehl GA, Gent P, Arblaster JM, Otto-Bliesner B, Brady E, Craig A (2001) Factors that affect amplitude of El Niño in global coupled climate models. Clim Dyn 17:515–526

Miyakoda K, Navarra A, Ward MN (1999) Tropical-wide teleconnection and oscillation. II: the ENSO-monsoon system. Q J R Meteorol Soc 125: 2937–2963

Navarra A, Ward MN, Miyakoda K (1999) Tropical-wide teleconnection and oscillation. I: teleconnection indices and type I/type II states. Q J R Meteor Soc 125:2909–2935

Parthasarathy B, Munot AA, Kothwale DR (1992) Indian summer monsoon rainfall indices: 1871–1990. Meteorol Mag 121:174–186

Rao KG and Goswami BN (1988) Interannual variations of sea surface temperature over the Arabian sea and the Indian monsoon. Mon Weather Rev 116:558–568

Rasmusson EM, Carpenter TH (1983) The relationship between the Eastern Pacific sea surface temperature and rainfall over India and Sri Lanka. Mon Weather Rev 111:517–528

Rayner NA, Parker DE, Horton EB, Folland CK, Alexander LV, Frich P (2000) The HadISST1 global sea–ice and sea surface temperature Dataset, 1871-1999. Hadley Centre Technical Note 17

Roeckner E, Arpe K, Bengtsson L, Christoph M, Claussen M, Dümenil L, Esch M, Giorgetta M, Schlese U, Schulzweida U (1996) The Atmospheric general circulation Model ECHAM4: model description and simulation of present-day climate. Max-Planck Institut für Meteorologie Report no.218 Hamburg 86 pp

Shukla J (1987) Interannual variability of monsoons. In: Fein JS, Stephenson PL (eds) Monsoons. Wiley, New York, pp 399–464

Shukla J, Fennessy MJ (1994) Simulation and predictability of monsoons. In: Proceedings of the International Conference on Monsoon Variability and Prediction Tech. Rep. WCRP-84 World Climate Research Program, Geneva, Switzerland

Soman MK, Slingo J (1997) Sensitivity of the Asian summer monsoon to aspects of sea surface temperature anomalies in the Tropical Pacific Ocean. Q J R Meteor Soc 123:309–336

Sperber KR, Palmer TN (1996) Interannual tropical rainfall variability in general circulation model simulations associated with the atmospheric model intercomparison project. J Clim 9:2727–2750

Sperber K, Hameed S, Potter JL, Boyle JS (1994) Simulation of the northern summer monsoon in the ECMWF model: sensitivity to horizontal resolution. Mon Weather Rev 122:2461–2481

Sperber KR, Slingo JM, Annamalai H (2000) Predictability and the relationship between subseasonal and interannual variability during the Asian summer monsoon. Q J R Meteor Soc 126:2545–2574

Stendel M, Roeckner E (1998) Impacts of horizontal resolution on simulated climate statistics in ECHAM4. MPI-Report 253:57pp

Terray P, Guilyardi E, Fischer AS, Delecluse P (2005) Dynamics of Indian Monsoon and ENSO relationships in a global coupled model. Clim Dyn 24:145–168

Trenberth KE, Stepaniak DP, Caron JM (2002) Interannual variations in the atmospheric heat budget. J Geophys Res 107(D8):AAC 4-1–15

Valcke S, Terray L, Piacentini A (2000) The Oasis coupler user guide version 2.4. Technical report TR/CMGC/00-10 CERFACS

Wang B, Wu R, Lau KM (2001) Interannual variability of the Asian summer monsoon: contrast between the Indian and the Western North Pacific–East Asian monsoons. J Clim 14:4073–4090

Webster PJ, Yang S (1992) Monsoon and ENSO: selectively interactive systems. Q J R Meteor Soc 118:877–926

Webster PJ, Magaña V, Palmer TN, Shukla J, Tomas RA, Yanai M, Yasunari T (1998) Monsoons: processes, predictability and the prospects for prediction. J Geophys Res 103:14 451–14 510

Xie P, Arkin P (1997) Global precipitation: a 17-year monthly analysis based on gauge observations, satellite estimates, and numerical model outputs. Bull Am Meteor Soc 78:2539–2558

Zhang R, Sumi A, Kimoto M (1996) Impact of El Niño on the East Asian monsoon: a diagnostic study of the '86–'87 and '91–'92 events. J Meteorol Soc Jpn 74:49–62